

**Directly Deposited Current Collecting Grids for AMTEC Electrodes**

M. A. Ryan, B. Jeffries-Nakamura, R.M. Williams,  
M.L. Underwood, D. O'Connor and S. Kikkari

Jet Propulsion Laboratory  
California Institute of Technology  
Pasadena, CA 91109

## ABSTRACT

Current collection in porous thin film electrodes on solid electrolytes has been improved by using thick film grids to decrease sheet and contact resistance in RhW and PtW electrodes. The grids are directly deposited on the solid electrolyte either by sputter- or photodeposition, and the electrode deposited over the grid. Comparison of the performance of electrodes having such underlying grids with that of electrodes without such grids has shown performance, as measured by current density power produced, to be improved by 10 - 30% in electrodes with grids.

## INTRODUCTION

Devices which use solid electrolytes, such as fuel cells, electrolysis cells or the alkali metal thermal-to-electric converter (AMTEC) often require that the electrode be porous in order to allow transport of vapor through the electrode from or to the electrolyte. The requirement of porosity in the electrode must, however, be balanced with the requirement of efficient electronic conduction. Thickening the electrode to enhance electronic conductivity may result in greatly impeding transport through the electrode, so an approach which will enhance conductivity while maintaining the ability for transport is desirable. The problem of maximizing both conductivity and transport in a metal electrode has been addressed by making a thin film, porous electrode which contains a thicker grid for current collection.

Electrodes which contain current collection grids have been made specifically for AMTEC, which is a direct energy conversion device, capable of near-Carnot efficiencies. The device is a sodium concentration cell which uses a ceramic, polycrystalline  $\beta$ -alumina solid electrolyte (BASE) tube as a separator between a high pressure region containing liquid sodium at 900 - 1300 K and a low pressure region containing a condenser at 400- 700 K. Sodium metal is oxidized at the liquid sodium/BASE interface and sodium ions are conducted through the BASE to the low pressure side of the BASE. Electrons travel through an external load to recombine with sodium ions at the interface between BASE and a thin film, porous metal electrode which has been deposited onto the low pressure side of the BASE; sodium vapor travels through the porous electrode, leaves the electrode as vapor and is collected on a cold condenser, from which it can be recirculated to the hot, high pressure side of the BASE.

[1,2].

Several studies on electrode materials for AMTEC have determined that rhodium-tungsten films co-sputtered approximately  $1.0 \mu\text{m}$  thick are among the best performing configurations. These films typically exhibit power densities of  $\sim 0.5 \text{ W/cm}^2$  [3,4]. Current collectors made of molybdenum mesh are overlaid on the electrode and tied off with molybdenum wires. It is necessary to use a current collector which will not impede sodium vapor flow as sodium leaves the electrode to condense on the cold surface; current collection networks have included wires spiraled over bus bars around the electrode [5], networks made of individual wires or of metal meshes or screen [4,6], and coarse felt or sponge [7].

Power density in an AMTEC electrode is lowered by resistance in the electrode (sheet resistance) and by resistance between the electrode and current collector (contact resistance). Reducing sheet resistance by thickening the electrode overall is not possible because of the need to maintain pathways for sodium vapor transport through the electrode. In order to improve the performance of the current collector, grids of molybdenum metal have been directly deposited on the BASF surface, and the porous metal electrode sputter deposited over the grids. These underlying grids are either sputter or photodeposited onto the BASF. The electrode is thus thickened in a grid pattern, lowering resistance in the thickened regions while maintaining the porosity of the electrode where there is no grid. Directly deposited grids have the advantages of being easily reproducible and requiring little additional handling of the ceramic. Other deposition techniques, such as painting, spraying or printing (in patterns) or sputter depositing over a photoresist mask are less suitable for time.

applications. Additional handling of the ceramic electrolyte raises the possibility of damage before use, and the electrolyte is sensitive to water, acid, CO<sub>2</sub> and ion exchange, so common solvents and reagents are not appropriate to use.

Photolytic chemical vapor deposition, or photodeposition, is a well established technique in the field of semiconductor (i.e. vice. fabrication and may be applied to deposition of metals and metal alloys on metal and insulating, substrates as well as to semiconductors [8-12]. It is accomplished at low pressure with an organometallic vapor, such as a metal carbonyl, surrounding the substrate. The substrate is masked or light is imaged in the pattern desired; the substrate is then irradiated with ultraviolet light. The organometallic compound dissociates as a result of absorption of UV light and metal condenses on the substrate surface in the illuminate area. It is possible to write patterns with micrometer resolution on the substrate using photodeposition [8,9,13].

Experiments lasting over 1000 hours in a sodium exposure test chamber (SETC) and in AMTEC cells have shown that at temperatures above 1000 K, electrodes with directly deposited grids consistently perform better than those without such grids. Both types of electrodes have tied-on mesh current collectors. Those with underlying grids have lower shed resistances and higher power densities. The power densities of electrodes with deposited grids are 15-35 % higher than those without, in spite of the thickened areas occluding sodium vapor transport. As AMTEC cells have recently been operated at efficiencies as high as 18% [14] and are projected to operate well in excess of 20% [15], this increase in electrode power density can result in an overall increase in device efficiency of ~5 %.

## EXPERIMENTAL

1.01  $\mu$ m crystalline ceramic  $\beta''$ -alumina tubes, 4.98-5.02 cm circumference, were purchased from Ceramatec, Inc. and prepared for use by firing in air at 1200 K for 4 hours. These tubes were masked in patterns with stainless steel foil or Kapton ribbons. Deposition of both photo- and sputter-deposited grids was done in two steps; the mask was placed in one direction (e.g. parallel to the c axis of the tube), the material deposited, then the substrate removed from the deposition chamber and masked in a perpendicular direction, to form a grid of interconnecting grid lines. After grid lines were deposited on the  $\beta''$ -alumina tubes, electrodes were deposited by magnetron sputtering. Electrodes were typically cylindrical in shape, 1 cm wide, for a total surface area of  $\sim 5$  cm<sup>2</sup>.

### *Photodeposition*

Molybdenum metal was deposited on the masked substrate using in an evacuated chamber equipped with a fused silica window, as shown in Figure 1. 100 mg of Mo(CO)<sub>6</sub> was placed in a separate chamber which was heated to 40 °C, which could be opened to the deposition chamber. The substrate was mounted on a rod containing a heater and the substrate heated to 120 °C. The sample chamber was evacuated, then opened to a flow of helium to bring the chamber pressure to  $\sim .5$   $\mu$ m. The helium flow was directed at the window to keep it clear of Mo(CO)<sub>6</sub>, in order to prevent photodeposition of Mo on the inside of the window. Helium carrier gas ( $p = .25$  torr) was flowed through the chamber containing Mo(CO)<sub>6</sub>. It was not possible to measure the Mo(CO)<sub>6</sub> pressure directly as the carbonyl will poison most pressure gauges; the pressure of Mo(CO)<sub>6</sub> at 40 °C is estimated to be  $\sim (0.07)$  torr. The sample chamber was

opened to the metal carbonyl chamber, bringing the total pressure to  $\sim 0.75$  torr. The full output of a 1000 W Xe-Hg lamp (Ilanovia) was directed through the window to illuminate the substrate. The power incident on the sample was measured as  $\sim 0.01$  W/cm<sup>2</sup> (200 - 250 nm).

The deposition rate of Mo from photodissociated Mo(CO)<sub>6</sub> on a 120 °C substrate was determined to be 5 μm/hour at 0.01 W/cm<sup>2</sup> of 200-250 nm radiation. The grid patterns on the cylindrical substrates used in these experiments were deposited in three segments, and so the tube was turned 120° after two hours of deposition. The result was a regular deposit approximately 10 μm thick, in a typical grid pattern, the lines were 2.50500 μm wide, defining rectangles of 6-8 mm<sup>2</sup>. For a cylindrical region 1 cm wide on the tube, an electrode area of  $\sim 5$  cm<sup>2</sup> was defined by a grid pattern. The lines of the grid represented some 15-20% of the electrode area. After deposition in both directions (⊥ c axis and // c axis) the BASF tube with Mo lines was annealed under vacuum with a zirconium foil getter at 1225 K for 4 - 6 hours. Annealing resulted in a loss of 10-20% of the grid height, resulting in lines  $\sim 8$  μm thick. The resistivity of the Mo lines was 50 μΩ-cm, or approximately 10 times the bulk resistivity of molybdenum. The grid lines were adherent, and could not be peeled off with adhesive tape or scraped off with a scalpel, either before or after annealing.

### ***Sputter Deposition***

Sputter deposited grids were made by masking the β"-alumina tube with adhesive tape to define the grid pattern. Because sputtering is not a line-of-sight process as is photodeposition, it was necessary to have the mask for

sputtered lines held firmly against the substrate surface. Kapton or paper tape which was adhesive on one side was used for the mask. After masking, the tube was placed on a rotating holder in a chamber for d.c. magnetron sputtering and sputtered with molybdenum using a 99.9% pure target. The first set of lines was sputtered 10  $\mu\text{m}$  thick. The substrate was removed and masked with a second set of adhesive tapes to make the cross line. The sputtered molybdenum did not adhere well to the  $\beta$ -alumina and was partially pulled up by the adhesive tape mask. However, after the second sputter, the resistivity of the grids was 200  $\mu\Omega\text{-cm}$ . The sputtered grids were not annealed.

### *Electrodes*

Rhodium tungsten and platinum tungsten electrodes were deposited on the  $\beta$ -alumina solid electrolyte tubes by cosputtering the two elements using d.c. magnetron sputtering, [16]. The tubes were masked to define electrodes 1 cm wide. A series of electrodes were put on each tube, some having underlying grids, some without.

Electrodes were wrapped in molybdenum screen which was tied on to the BASF tube with Mo wire. Molybdenum wire leads were attached to each electrode and insulated with 99.8%  $\alpha$ -alumina ceramic tubes. Electrodes with underlying grids were compared to electrodes without grids in two configurations, in a Sodium Exposure Test Cell (SETC) and in a full AMTEC experiment.

### *Sodium Exposure Test Cell*

The Sodium Exposure Test Cell (SETC) consists of a stainless steel

chamber with a flange containing six feedthroughs for leads and thermocouples and a heater well which goes the length of the chamber, down the center. A diagram of the SETC is shown in Figure 2. A section of BASF tube with four 5 cm' electrodes was mounted on the heater well. The heater well was insulated with u-alumina, electrically isolating the BASF from the chamber. The chamber was sealed and evacuated, and 20 grams of sodium metal added after evacuation. The chamber was put in a tube furnace and the entire assembly elevated at one end so the liquid sodium would stay in contact with the flange, which was wrapped in a heating tape for temperature control of the liquid sodium. By heating the furnace and placing a heater in the heater WC.], the BASF tube could be kept at a constant temperature, with a gradient across all four electrodes of no more than 5 K. The sodium pressure in the chamber could be controlled by the temperature of the flange with which the sodium was in contact.

The four electrodes on the BASF were a pair with underlying grids and a pair without. The pairs were operated as a two electrode electrochemical cell, using a PAR 173 potentiostat with a PAR 193 Universal Programmer for applying a potential ramp. Each electrode in a pair was operated as both an anode and a cathode by changing the potential between them.

Electrochemical impedance spectroscopy (EIS) studies were made on each pair using a set-up which has been previously described [4]. A model which allows determination of electrode performance parameters analogous to those defined for electrodes in an AMTEC cell [3,4] was developed. Performance parameters determined include  $R_{act}$ , the apparent charge transfer resistance;  $B$ , the temperature-independent exchange current;  $G$ , a dimensionless morphology parameter which reflects impedance to sodium flow through the electrode; and

the current measured in an iV curve. The model may be used with electrochemical impedance spectra or with iV curves, and has been presented in detail in a report from JPL. [17].

### ***AMTEC Experiment***

After testing grid components in the S1 iFC, a BASF tube was prepared for an AMTEC experiment. The experimental set-up and methods of data analysis have been previously described [4,6]. In order to compare electrodes with grids with those without grids, a BASF tube was prepared for an AMTEC experiment with six 5 cm<sup>2</sup> electrodes. Four of those electrodes had underlying grids, two did not. One of the electrodes with a grid was contacted by tying a single molybdenum wire around it. The other five electrodes were contacted by tying molybdenum screens over them with Mo wire, and attaching a Mo wire lead.

### **RESULTS AND DISCUSSION**

For efficient operation in solid electrolyte cells such as AMTEC, current of a few Amps/cm<sup>2</sup> and equivalent gas fluxes are required while iR losses must be quite low. For example, an AMTEC cell operating at 0.5 W/cm<sup>2</sup> (1.0 A/cm<sup>2</sup> and 0.5 V) may have an internal ohmic component of resistance of 0.4 Ω-cm<sup>2</sup>. A change of 0.1 Ω-cm<sup>2</sup> at the same current density would change the power and efficiency by 20% relative to initial power and efficiency levels. The effect of small ohmic resistances is less significant in higher voltage, lower current devices. The overall effect of changes in electrode sheet resistance in a device such as AMTEC can be significant [4,6], and it is those effects which are largely

responsible for the performance improvements made in this study. Calculations of current and voltage profiles across thin film electrodes with sheet resistances of some  $10 \Omega/\square$  in cylindrical and circular grid geometries have been reported previously [4,6]. These calculations showed that in the case of 1 mm radius circular grid elements, for a grid voltage of 0.4 V (typical peak power voltage for an AMTEC electrode), the current density would decline - 30% from the perimeter to the center of the circular electrode element. Placement of grids can, then, prevent loss of current carrying capability in electrodes.

A full description of the effects of underlying grids on electrode performance requires determination of performance parameters which may be extracted from experimental data, as well as the sheet resistance ( $R_{sh}$ ) measured before and after the experiment, and the specific power during operation. Those parameters which may be measured directly are apparent charge transfer resistance ( $R_{act}$ ), sheet resistance ( $R_{sh}$ ) and lead and contact resistance; those which are derived using the model are temperature-independent exchange current ( $B$ ), and the morphology factor ( $G$ ). Each of these parameters may be determined from an AMTEC experiment Or from an SETC experiment, using either current-voltage curves or electrochemical impedance spectroscopy. The model for calculation of these parameters from AMTEC cell data and from EIS on an AMTEC cell has been previously discussed in detail [4, 18]. Such a model has also been developed at JPL for analysis of SETC data [ 17].

The derived parameters are not fully independent, as a high sheet resistance has the effect of reducing the active electrode area to that near the current conduction network (grid line or lead), and reducing  $B$  while increasing  $G$  with respect to their "true" or absolute values for the electrode film. The

morphology factor,  $G$ , is a dimensionless parameter which scales linearly with the impedance to sodium vapor flow from the reaction region at the electrode/electrolyte interface to the condenser. It may be derived from BIS in an AMTEC cell or from the observed limiting currents in SETC cell current-voltage curves. The charge transfer resistance  $R_{ct}$  and the exchange current  $B$  correspond to standard electrochemical terms. In an SETC cell they may be derived from the slope of the current-voltage curve about 0.0 V, taken at low sodium pressure.

#### *Sputter Deposited Grids, Rh W Electrodes*

A set of experiments, an SETC and an AMTEC experiment, was done with rhodium tungsten electrodes and sputter deposited Mo grids underlying the electrode. Table I shows several characteristics of electrodes before, during and after the AMTEC experiment,

Before operation, the sheet resistance for electrodes with grids was lower than sheet resistance in electrodes without grids. The improved sheet resistance is reflected in the lower  $R_{act}$  and higher  $B$  found in grid electrodes.  $G$ , the morphology factor which is an indicator of impedance to sodium transport through the electrode is higher in grid electrodes than in electrodes without grids. As 15-20 % of the projected area of an electrode is occluded to sodium flow by the 8  $\mu\text{m}$  thick grid lines, it is not surprising that sodium flow is somewhat inhibited in electrodes with grids. Nevertheless, as seen in Figures 3 and 4, overall performance for electrodes with grids was superior to that of electrodes without grids. The electrodes in the AMTEC experiment were contaminated with copper, which alloyed with Rh in the electrode and formed an intermetallic,

resulting in a high sheet resistance after 800 hours of operation.

Figure 3 shows a comparison of electrode performance in the SETC. It is a plot of the ratio of measured or calculated electrode performance parameters vs. time, where the ratio is that of grid performance to no-grid performance. The electrodes were held 1125 K and the sodium pressure within the chamber was  $2 \times 10^{-4}$  Pa for all joints. Three performance parameters are included: current at 1 V,  $R_{act}$ , and G. The current for electrode pairs with underlying grids was consistently higher than current for pairs without grids; the average current difference was 20%. This current difference has been corrected for electrode area and for the distance between electrodes in a pair.  $R_{act}$  in the electrodes with grids was consistently lower than  $R_{act}$  in electrodes without grids, indicating lower resistance in the electrode. The morphology factor G was consistently higher in electrodes with grids, indicating poorer sodium transport in those electrodes, which would be expected in electrodes with occluded regions.

In an AMTEC experiment using sputter deposited grids, power produced was consistently higher for electrodes with both grids and overlying mesh. Figures 4a and 4b show plots of maximum power vs. time and power vs. temperature for two electrodes in the cell. After the initial maturation of electrodes, the maximum power for the electrode with the underlying grid was, on the average, 30% greater than the power for the electrode without the grid. The power levels compared in Figure 4a were produced at temperatures from 1050 - 1125 K. Note in Figure 4b that the temperature of the non-grid electrode was somewhat higher than the temperature of the grid electrode, but that in spite of the lower temperature, the grid electrode had higher power. The electrode which had an underlying grid and a single molybdenum wire lead had maximum power about

10% lower than mesh-contacted electrodes without underlying grids. Current collection networks including meshes capable of carrying high currents are important in cells with current densities of  $-1 \text{ A/cm}^2$  and greater, as is the case with AMTEC cells.

Scanning Electron Microscopy (SEM) done after the SETC and AMTEC experiments showed that there was no measurable migration of the sputtered molybdenum grids into the RhW electrode material, although grain growth in the Mo grid area was faster than in areas without grids. This increased rate of grain growth is consistent with measured surface self-diffusion coefficients which show Mo to diffuse 1 to 2 orders of magnitude faster than  $\text{Pt}_{2.5}\text{W}$  and  $\text{Rh}_2\text{W}$  at 1125 K [19]. The gridlines were not adherent, and upon removal of the BASE from the cell, flakes of molybdenum plus Rh W electrode could be seen separating from the electrolyte. This flaking was consistent with the observation before the experiment that the grid lines could be lifted from the solid electrolyte with adhesive tape. The relatively high sheet resistance in the electrode is attributed to flaking and buckling of sputter deposited grid lines during operation.

### *Photodeposited Grids, Pt W Electrodes*

An SETC experiment was run to compare pairs of  $\text{Pt}_{2.5}\text{W}$  electrodes with and without underlying, photodeposited molybdenum grids. As in the case of sputter deposited grid lines, the initial sheet resistance of electrodes with grids was lower than that of electrodes without grids. Figure 5 shows ratios of current at 1 V and  $R_{act}$  for grid/no grid electrodes.  $\text{Pt}_{2.5}\text{W}$  electrodes have excellent sodium transport characteristics, and there was no apparent impedance to sodium flow in either grid or no-grid electrodes ( $G=0$ ) at the experiment temperature of 1125

K. In an experiment lasting -1300 hours, electrode pairs which had underlying current collection grids consistently had higher currents than pairs which did not have such grids. During the first 50- 100 hours, the electrode pair with grids improved its performance, while the pair without declined slightly. The improvement in performance early in life is attributed to a lowering of contact resistance between grid lines and electrodes as Mo and  $Pt_{2.5}W$  grains conform to each other at high temperature and as any impurities (e.g. oxides) in the grid lines are removed by sodium in the electrode. After 500 hours, and until the experiment was turned off at 1300 hours, the grid electrode pair carried 10% more current than the pair without grids. The resistance in the electrodes followed a similar pattern.

## CONCLUSION

Grid lines occluding some 15-20% of the surface of a porous electrode on a solid electrolyte can be used to improve the electrical characteristics of the electrode, resulting in overall improvement of performance in a cell. It was found that the mechanical characteristics of grid lines deposited by photolytic chemical vapor deposition were superior to those deposited by sputter deposition, in that they are adherent and do not flake off the solid electrolyte under operation. Performance, as measured by  $R_{act}$  and by current-voltage behavior, was somewhat better in sputter deposited grids than in photodeposited, possibly because of CO or carbon inclusions in photodeposited grid lines.

Experiments are underway at JPL to investigate various aspects of current collecting grids. These aspects include determination of the optimum line width to minimize G, and different contacting configurations to eliminate the need for

4

tied-on meshes. We are also investigating the possibilities of directly depositing grids which overlay the electrode and its underlying grid and in making grids which are integral with the electrode; *i.e.* made simultaneously with the electrode.

#### ACKNOWLEDGEMENTS

The research described in this paper was carried out by the Jet Propulsion Laboratory, California Institute of Technology, under a contract with the National Aeronautics and Space Administration. It was supported by the National Aeronautics and Space Administration, the Air Force Phillips Laboratory and the Department of Energy.

## REFERENCES

1. N. Weber, *Energy Conv.*, **14**, 1 (1974).
2. T.K. Hunt, N. Weber and T. Cole., *Proc.10th Intersociety Energy Conv. Engineering Conf.*, **3**, 231 (1975).
3. R.M. Williams, B. Jeffries-Nakamura, M. I. Underwood, B.L. Wheeler, M. II. Loveland, S.J.Kikkert, J.L.Lamb, T. Cole, J.T. Kummer and C.P. Bankston, *J. Electrochem. Soc.*, **136**, 893 (1989).
4. R.M. Williams, M.E. Loveland, B. Jeffries-Nakamura, M. I. Underwood, C.P. Bankston, H. I educ and J .T.Kummer, *J. Electrochem. Soc.*, **137**, 1709 (1990).
5. N. Weber, *Energy Conversion*, **14**, 1 (1974).
6. B.L. Wheeler, R.M. Williams, B. Jeffries-Nakamura, J.L. Lamb, M.E. Loveland, C.P. Bankston and T. Cole, *J. Appl. Electrochem.*, **18**, 410 (1988).
7. K. Tanaka, A. Negishi and T. Masuda, *Proc. 27th Intersociety Energy Conversion Engineering Conf.*, T. Bland, ed., *Society of Automotive Engineers*, Warrendale, PA (1992) Vol 1, pp. 13-18.
8. Dieter Baeuerle, *Laser Processing and Diagnostics*, Springer-Verlag, Berlin, 1984.
9. D.J. Ehrlich, R.M. Osgood and "I". F. Deutsch, *J. Vac. Sci. Technol.*, **21** (1982),
10. G.A. Kovall, J.C. Matthews, and R. Solanki, *J. Vac. Sci. Technol. A*, **6**, 2353 (1988).
11. R.M. Osgood and T.F. Deutsch, *Science*, **227**, 709 (1985).
12. Y.R. Froidevaux, R.P. Salathe, H .H. Gilgen, "I aser Diagnostics and Photochemical Processing for Semiconductor Devices", R. M. Osgood, S.R.J.

- Grueck and H.R. Schlossberg, eds., North Holland, New York (1983).
13. K.A. Singmaster, F.A. Houle and R. J. Wilson, *J. Phys. Chem.*, **94**, 6864, (1990).
  14. T.K. Hunt, Advanced Modular Power Systems, Inc.; unpublished results (1994).
  15. T. Cole, *Science*, 221,915 (1983).
  16. R.M. Williams, G. Nagasubramanian, S.K. Khanna, C.P. Bankston, A.P. Thakoor and T. Cole, *J. Electrochem. Soc.*, **133**, 1587 (1986),
  17. M.A. Ryan, R.M. Williams, B. Jeffries-Nakamura, M.I. Underwood and D. O'Connor, JPL New Technology Report NPO-18620; *NASA Tech Brief*, 17(9), 80 (1993).
  18. R.M. Williams, B. Jeffries-Nakamura, M.I. Underwood, C.P. Bankston and J.T. Kummer, *J. Electrochem. Soc.*, **137**, 1716 (1990).
  19. M.A. Ryan, A. Kisor, R.M. Williams, B. Jeffries-Nakamura, and D. O'Connor; *Proc. 29th Intersociety Energy Conversion Engineering Conference*, R. Winn, ed., American Institute of Aeronautics and Astronautics, Vol. pp (1994).

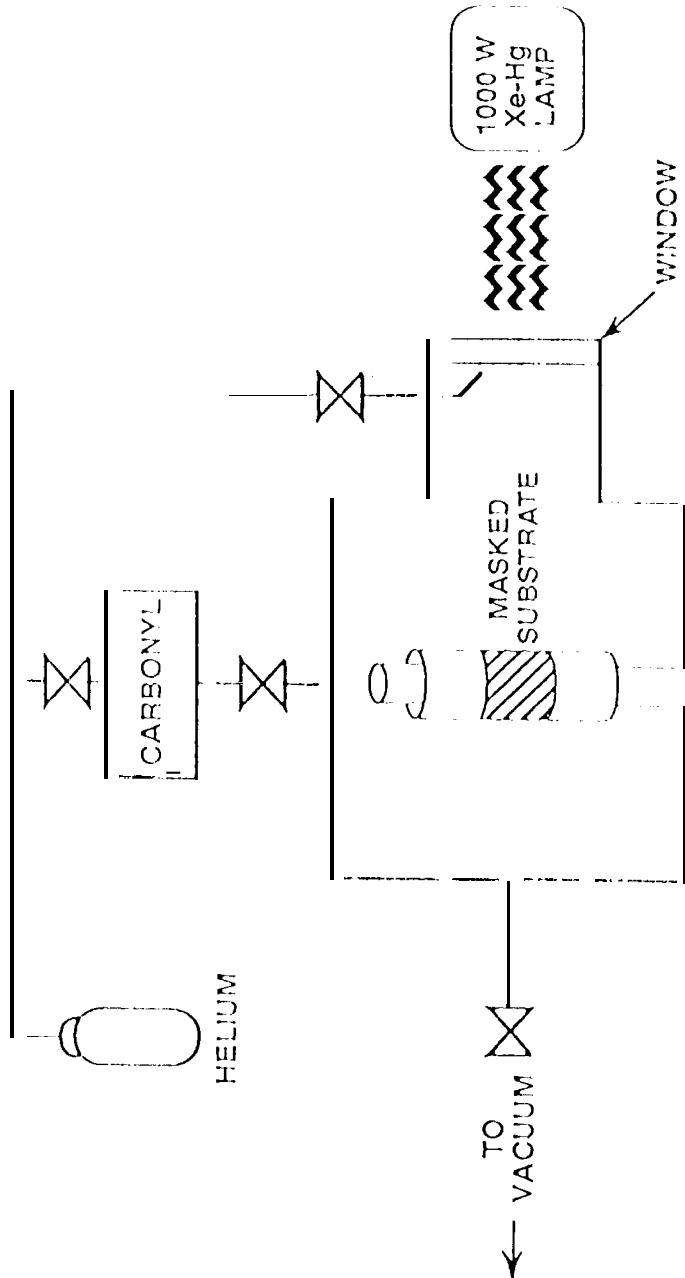
TAB I EI

	$R_{sh, 000}$	$R_{sh, 800}$	$R_{act, 50}$	$R_{act, 400}$	$B_{50}$	$B_{400}$	$G_{50}$	$G_{400}$
	$\Omega/[]$	$\Omega/[]$	n	n	AK/mPa	AK/mPa		
GRID	1.4	9.0	1.8	1.6	112	57	7.2	8.2
NOGR	9.6	9.4	3.0	2.2	77	29	4.8	6.9

Table I: Characteristics of RhW electrodes with and without sputtered Mo grids in an AMTEC experiment, before, during and after an 800 hour experiment.  $R_{sh}$  - sheet resistance at 0 and at 800 hours;  $R_{act}$  - charge transfer resistance at 50 and at 400 hours;  $B$  - temperature independent exchange current at 50 and 400 hours;  $G$  - morphology factor at 50 and 400 hours

## 1.1ST OF FIGURES

1. The set-up of photolytic chemical vapor deposition using a Xe-Hg lamp.
2. The Sodium Exposure Test Cell (SETC); (a) refers to vacuum-tight feedthroughs for electrically isolated electrode leads, and (b) refers to feedthroughs for thermocouples and other monitoring devices.
3. Ratios of current at 1 V (0),  $R_{act}$  ( $\nabla$ ), and G ( $\blacklozenge$ ) of grid to no grid electrodes operated in an SETC at 1125 K, plotted vs. time. Sputter deposited Mo grids under sputtered  $Rh_2W$  electrodes.
- 4a. Ratios of maximum power (0) and of  $R_{act}$  ( $\blacklozenge$ ) of grid to no grid electrodes operated in an AMTEC cell,  $T = 1100$  K. Sputter deposited Mo grids under sputtered  $Rh_2W$  electrodes.
- 4b. Maximum power of grid ( $\blacklozenge$ ) and no grid (0) electrodes operated in an AMTEC cell, plotted vs. temperature. Electrodes with grids produced higher power at lower temperatures.
5. Ratio of current at 1 V (0) and of  $R_{act}$  (\*) of grid to no grid electrodes operated in an SETC at 1125 K, plotted vs. time. Photodeposited Mo grid lines under sputtered  $Pt_{2.5}W$  electrodes.



HEATER  
&  
SUBSTRATE SUPPORT

